energies

MDPI

Article

Development of a Self-Calibrated Embedded System for Energy Management in Low Voltage

Eder Andrade da Silva [1,2,*], Carlos Alejandro Urzagasti [1,2], Joylan Nunes Maciel [1,2], Jorge Javier Gimenez Ledesma [1,2], Marco Roberto Cavallari [2,3] and Oswaldo Hideo Ando Junior [1,2,4]

1 Latin American Institute of Technology, Infrastructure and Territory (ILATIT), Federal University of Latin American Integration (UNILA), Foz do Iguaçu 85867-000, PR, Brazil
2 Research Group on Energy & Energy Sustainability (GPEnSE), Pernambuco 54518-430, PE, Brazil
3 School of Electrical and Computer Engineering (FEEC), State University of Campinas (Unicamp), Campinas 13083-852, SP, Brazil
4 Academic Unit of Cabo de Santo Agostinho (UACSA), Federal Rural University of Pernambuco (UFRPE), Cabo de Santo Agostinho 54518-430, PE, Brazil
* Correspondence: ea.silva.2020@aluno.unila.edu.br; Tel.: +55-(48)999927750

Abstract: Due to the growing concern and search for energy sustainability, there has been an increase in recent years in solutions in the area of energy management and efficiency related to the Internet of Things (IoT), the home energy management system (HEMS), and the building energy management system (BEMS). The availability of the energy consumption pattern in real time is part of the necessity presented by this research. It is essential for perceiving and understanding the savings opportunities. In this context, this manuscript presents the development of a self-calibrated embedded system to measure, monitor, control, and forecast the consumption of electrical loads, enabling the improvement of energy efficiency through the management of loads performed by the demand side. The validation of the produced device was performed by comparing the readings of the device with the readings obtained through the evaluation system of the integrated circuit manufacturer ADE9153A®, Analog Devices® purchased in Brazil. The result obtained with the developed device featured errors smaller than ±0.1%, which were in addition smaller than ±1% with respect to the full scale, thus proving to be a viable solution for the proposed application.

Keywords: energy meter; energy savings; IOT; self-calibrated; load forecasting; building energy management system (BEMS); home energy management system (HEMS)

Citation: Silva, E.A.d.; Urzagasti, C.A.; Maciel, J.N.; Ledesma, J.J.G.; Cavallari, M.R.; Ando Junior, O.H. Development of a Self-Calibrated Embedded System for Energy Management in Low Voltage. *Energies* **2022**, *15*, 8707. https://doi.org/10.3390/en15228707

Academic Editor: Angelo Zarrella

Received: 27 September 2022
Accepted: 16 November 2022
Published: 19 November 2022

1. Introduction

Technological advances in recent decades have allowed for monitoring of energy consumption patterns in real-time. This monitoring is essential to provide opportunities for rationalization of energy consumption, a thought that meets the search for sustainable processes and technologies aimed at promoting energy efficiency and sustainability. Among the aspects that make it possible to achieve this purpose, the concept of smart buildings stands out. This denomination arises with the increase in the integration of advanced technology in buildings and their systems so that the entire operating cycle of buildings can be operated and controlled remotely for convenience, comfort, economy, and energy efficiency [1–3].

Approximately 40% of global energy consumption is attributed to urban buildings, which contribute to 30% of the world's total CO_2 emissions [4]. Still in terms of sustainability, global greenhouse gas emissions are continuously growing on a worldwide scale and climate change issues are increasingly present, causing serious impacts on populations and the environment [5].

All around the world, countries are looking for alternatives to the challenge of building decarbonization in the coming years and the proposed policies for this include: increasing

the proportion of buildings with almost zero energy requirements, Nearly Zero Energy Buildings (NZEB); smarter and more efficient energy systems; and behavioral changes in energy consumption by consumers [4].

The integration of the Internet of Things (IoT) in smart buildings is one of the means to achieve these goals, in order to enable real-time measurements and information with relevant data [6]. Applications in lighting, the use of household appliances, vehicle parking, and access authorization, among others, can be recognized and controlled by the use of objects connected to the same network [7].

Currently, the concept of the IoT is consolidated as the environment of people and objects interconnected with each other, not just dealing with machine-to-machine (M2M) communication. The IoT is about much more, it's about the way humans and machines connect, using common public services [1].

Therefore, this work presents the development of a self-calibrated, Class 1, embedded system for metering, consumption monitoring, and load control. In addition to these functionalities, a load forecasting module based on artificial intelligence techniques [8] was developed, evaluated, and integrated into the embedded system, enabling the improvement of energy efficiency through demand side management. The innovation of the device is given by the use of the ADE9153®, which, being a self-calibrated chip, reduces the calibration costs through self-calibration of the metrology. In addition, something that is noteworthy is the chip's ability to provide the waveforms of the signals in the instantaneous current and voltage channels processed by the DSP at 4kSPS. The solution developed in this study is relevant especially to countries such as Brazil, in which there is a scarcity of studies, proposals and in particular information related to the consumption, demand and, prediction of residential energy load. Compared to the competing pieces equipment on the market, the system has a competitive financial cost, provides a larger set of functionalities, and includes a differentiated solution in terms of the scalability of the management and monitoring system [9–11].

Background and Related Works

The bibliographic survey was carried out using the Methodi Ordinatio [12]. This methodology takes into account the three most relevant factors to be considered in the search for a paper: (*i*) the year of publication of the article; (*ii*) the number of citations that the paper obtained until the date of the research; and (*iii*) its impact factor.

With the implementation of the methodology, papers with relevance and adherence to the subject of the research were selected to compose the bibliographic portfolio of this paper. Due to the subject of the research being the development of electronic equipment, some development documents and manuals of electronic equipment used in the circuits and relevant to the research were also included as a reference.

Some of the most recent prototypes among the devices in the surveyed portfolio are presented below. In [13], the authors present the development of an IoT, a low-cost smart energy meter. This meter features 2018 hardware capable of adapting to network variability while maintaining a high level of measurement accuracy. The prototype presented has an IC ADE7913®, fully isolated, analog-to-digital converter (ADC) designed for a variety of applications, among them, power measurement. The ADE7913® performs the necessary calculations and transfers the values via SPI (serial interface) to a STM32F2® microcontroller from STMicroelectronics®, which in turn transfers the data to a Texas Instruments® RF transceiver operating at a communication frequency of 169 MHz.

In [14], the authors presented an automation system using the HLW8012® energy meter from HLW Technology® and an IC ESP8266® of the Espressif Systems®, responsible for reading the pulses generated by the energy meter and sending the calculated consumption to a gateway through of the message queue telemetry transport (MQTT) protocol. Such technology allows the activation of load control relays through an internet browser on a computer or cell phone.

In more recent studies such as in [15], methodologies of real-time monitoring systems for estimating consumption are being developed. The proposed methodology comprises three main parts: (*i*) an event detection system to find active power changes corresponding to turn-on events; (*ii*) a CNN binary classifier to determine if the turn-on event was caused by a specific target appliance or not; and (*iii*) a power estimation algorithm to calculate in real-time the appliance power per second and, consequently, the energy consumption. Complementarily, reference [16] presents a computationally efficient and scalable refinement of the previous solution that eliminates the need for training.

A proposed improved model for the building energy management system (BEMS) is presented in [17], containing flexibility to respond to environmental conditions that results in less energy consumption. Forty-six swarm intelligence algorithms are used to evaluate the performance of the proposed model and it has been evaluated economically with and without BEMS.

The study presented in [18] reveals the development of a remote sensing technology compatible with an in-situ measurement implemented at Palazzo Tassoni (Italy). The electronics for environmental parameter measurement is composed of sensor measurements, a data acquisition system, and a data storage and communication system. The data acquisition system, equipped with standard Modbus-RTU interface, is designed to run autonomously, and is based on two cloned single board PCs to reduce the possibility of data loss. The storage and communication systems are based on an industrial PC that communicates with the sensor measurement system via a Modbus-TCPIP bridge.

In [19], a simple but cost-effective hardware and software solution was implemented targeting an outdated air conditioning system without voiding the warranty of the outdated equipment and without installing any additional measures. The proposed operation is designed to be easy to operate under the limitation of equipment and unskilled labor, and the indoor temperature schedules during the DR event are provided with some public data sets to determine the capability of the energy management system to reduce energy consumption in the office building without any effect on occupant comfort. The actual operation of the proposed solution can achieve the maximum power reduction 43.79% of the maximum power consumption while maintaining only 1 °C difference from the typical ambient temperature (26–28 °C).

In addition to the bibliographic portfolio search, a search for patents of similar devices to the proposed system, was carried out in the patent database of the Brazilian National Institute of Industrial Property (INPI).

The INPI database provides an overview of developments in the Brazilian national territory on the topic addressed, although the database also contains international patents. To carry out the searches, the following terms were addressed in titles and abstracts: (i) energy meter; (ii) energy efficiency; and (iii) IoT.

The search resulted in nine patent records for products related to the object of this work, four with the term energy meter, four with the term energy efficiency, and one with the term IoT.

Of these, the three most recent are BR 10 2019 023392 3, with the title: "Device integrated with management, automation, monitoring, consumption control and electricity quality for residential, commercial and industrial electrical distribution boards based on the Internet of Things", which differs from the proposed prototype because it is arranged in master–slave modules and does not have self-calibration [20].

BR 10 2018 017224 7, entitled "System for remote management of electrical loads", which differs from the proposed prototype as it requires an additional background system on a local computer, or a virtual machine stored in the Cloud to function [21].

And BR 10 2017 025250 7, "Device and system for monitoring the efficiency of electrical equipment", which differs from the proposed prototype as it requires a server to concentrate data on site [22].

Based on the analysis of the main scientific studies and patent registrations, no proposal was identified using the ADE9153A® data acquisition chip, which, because it is a

self-calibrating chip, allows the reduction of device calibration costs and performs the metrological calibration by itself. In addition, no similar devices (patent or product) were identified or used in Brazil, a country that has a large absence of information related to residential energy consumption.

In this context, this study aimed to develop a system composed of a user-friendly interface connected to a self-calibrated energy meter, including the management of devices, users, parameterization and remote control, interoperability between the devices, data storage, processing and decision making, as well as power quality analysis [23]. In addition to these functionalities, an additional module using deep learning [24] for household energy consumption forecasting (HECF) has been developed, evaluated, and composes the proposed system.

Therefore, the developed system is an electronic metering and electronic remote-control device with a cost of around 300 BRL (i.e., around 60 USD at the current exchange rate), that through portable electronic devices, allows the user to monitor their energy consumption and carry out the control of low voltage single-phase loads in a friendly interface. Its installation makes measuring and controlling loads simple, helping to reduce wasted energy consumption and control demand.

It is worth mentioning that the developed device is not just a residential power consumption monitoring meter, but it can have a sampling function of current and voltage signals up to 4kSPS to enable the detection of the load type through post-processing, functionality which also serves to detect faults in circuits.

2. Materials and Method

To carry out the system development, it was necessary to determine the characteristics of availability of purchase in the market, agility of development, processing capacity, and wireless connection.

After performing the analysis, the ESP32® microcontroller module from Espressif Systems® was selected as a way to develop a prototype [25].

Among the manufacturers surveyed, the one with the greatest availability of chips in the electrical energy measurement segment and with possible characteristics for the projected development, added to the availability of evaluation boards, was an Analog Devices® [26].

Considering the available options by the manufacturer, the ADE9153A® was selected because it is the only single-phase meter integrated circuit which is self-calibrated. This resource was considered a determinant when choosing the integrated circuit, as none of the surveyed competitors had it when carrying out this work [27].

To select the hardware, the specifications of the necessary characteristics were delimited and to meet mainly residential loads, the operating range of the system was specified as single-phase from 85 V to 250 V and up to 10 A. The communication via wireless networks and data acquisition accuracy were of at least 1%. With these definitions, the hardware prototype was divided into functionality blocks, making it modular (see Figure 1).

The device firmware was developed using the Arduino® programming platform and the dashboard for data monitoring and load control was developed using the IoT ThingsBoard® platform.

To enable access in a simplified, reliable, and twenty-four-hour way, the ThingsBoard® platform was installed on a Google Cloud Platform® (GCP) virtual machine. The device's communication with the GCP is carried out through the MQTT communication protocol. MQTT is an optimized messaging protocol for sensors and small mobile devices.

The MQTT protocol was chosen because it was specifically developed for communication between remote devices, due to its ease of implementation, low bandwidth allocation, quality of service (QoS), and higher level of security.

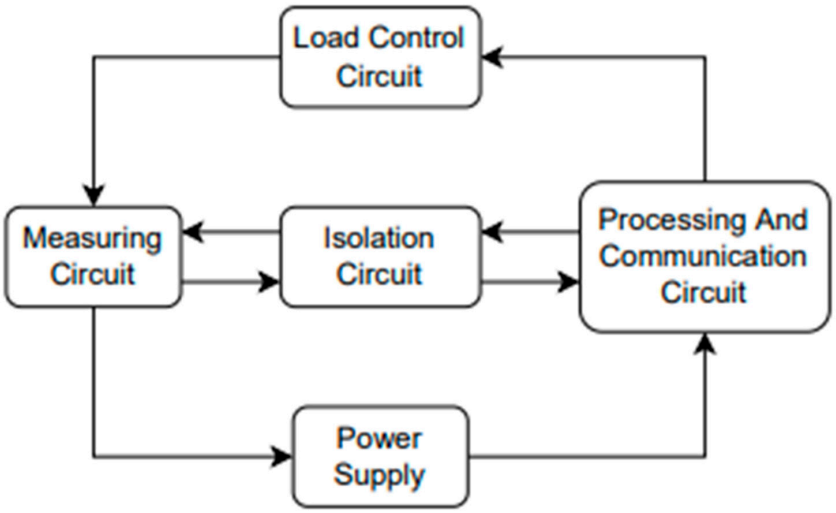

Figure 1. Hardware flowchart.

2.1. Measuring Circuit

The single-phase energy measurement IC with self-calibration was added to the project in order to guarantee the reliability of the measurements performed.

It incorporates three analog-to-digital converters, providing a signal-to-noise ratio of 88 dB and a set of advanced metrology features such as calculation of active power, fundamental reactive power, and apparent power, as well as RMS voltage and current calculations. The voltage and current channels ADC waveforms can be sampled at 4kSPS. The chip also includes power quality measurements such as zero crossing detection, line period calculation, angle measurement, peak detection, overcurrent, and power factor measurements.

The selected sensors were a 0.5 mΩ shunt resistor-type electrical current sensor and a resistive divider-type voltage sensor, composed of four 249 kΩ resistors in a series as a large resistor and a 1 kΩ resistor as a small resistor, all with 1% tolerance. This option was due to the fact that these resistors have measurement quality, reliability, reduced production costs, and ease of development.

In order to adjust the supply voltage to 3.3 V, a voltage regulator was supplied exclusively to the ADE9153A®, a feature used in conjunction with the insulation board to ensure isolation and noise suppression between the voltage sources of the measurement boards and processing.

With the components defined, it was possible to develop the layout of the board in a surface mounted device (SMD). The measurement board was produced in fiberglass with a thickness of 1.6 mm and a double copper face, as shown in Figure 2.

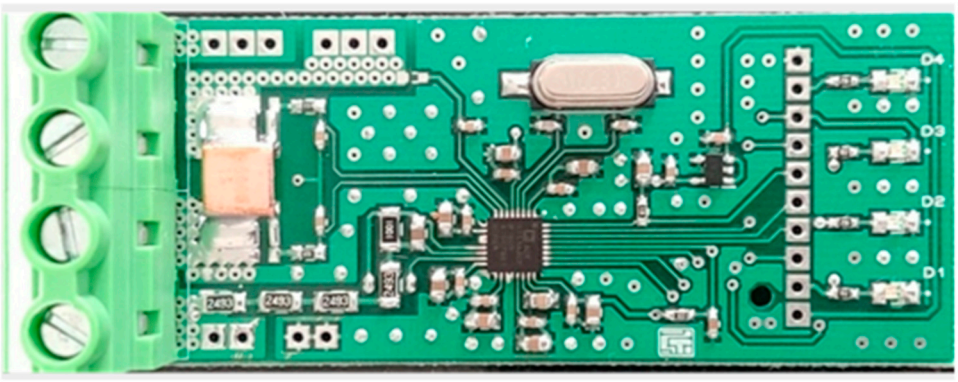

Figure 2. The measuring circuit board.

2.2. Isolation Circuit

To ensure the security and integrity of the information transmitted, all connections between the boards were made with isolation circuits. The most critical connection is between the measurement and data processing boards, due to the number of vias used and the speed of communication between the components. Therefore, for this part of the circuit, the IC ADuM4152BRIZ® and the IC ADuM6000ARIZ®, both from Analog Devices®, were used.

The ADuM4152BRIZ® is a digital isolator for a serial peripheral interface (SPI) that operates at 5 V or 3.3 V, has 5 kV isolation for 1 min, 25 kV/µs transient immunity, and supports SPI speeds up to 17 MHz.

The ADuM6000ARIZ® is a 400 mW isolated DC-DC converter that operates at 5 V or 3.3 V, has 5 kV isolation for 1 minute, and transient immunity of 25 kV/µs that was developed to work together with the previous one, allowing complete isolation of lines data and power.

The isolation circuit board, like the other boards, was produced in fiberglass and double-faced copper, it is relatively simple as it only needs the connection terminals and some coupling capacitors to avoid interference.

2.3. Processing and Communication Circuit

To enable wireless communication, the ESP32® module was defined as the prototype controller. The selected controller has Wi-Fi 802.11 b/g/n and Bluetooth v4.2 BR/EDR and BLE as wireless connectivity. It also has the SPI interface for communication with the ADE9153A® and input pins for the 32 kHz crystal used as a time base for the real-time clock, programmable set buttons, reset facilities, boot facilities, and an output to enable the activation of the charge.

In the same way as in the measurement circuit, the processing and communication circuit has a linear regulator of 3.3 V. However, due to the current peak when starting the communication, the IC used is the LM1117MP-3.3® of the Texas Instruments® which together with the capacitors provides enough power for the ESP32® to operate without failing, with wireless communication, and immunity to interference, thus avoiding having to be reset due to power a supply voltage drop as indicated by Espressif Systems®.

The prototype also provides data storage on a memory card provided in the hardware and the processing circuit was designed to be expandable through the universal asynchronous receiver transmitter (UART) communication port. The latter also serves to perform the firmware update when a wireless update is not possible. The UART is also used for debugging through serial communication.

The layout was developed in a double face with the components allocated in a single face. This practice was selected to speed up the production process in scale through SMD pick and place machines.

The cutout in the metallic part of the board and the positioning of the antenna of the communication circuit were developed observing the chip manufacturer's recommendations. In Figure 3, the 3D visualization generated from the layout developed for the processing board can be observed.

As with any communication circuit, the supply voltage regulation is very close to the chip's supply point, providing robustness and noise immunity.

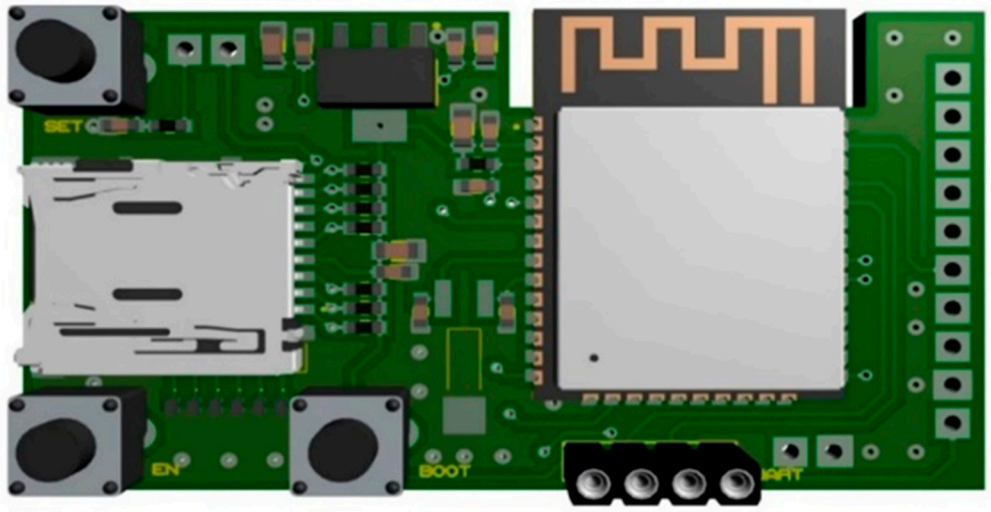

Figure 3. Processing and communication circuit board.

2.4. Power Supply

Due to the need of miniaturization and to automatically operate at 110 V or 220 V, the power supply was designed as an isolated flyback switching power supply. The power supply uses the TNY268® of Power Integrations® as a switching circuit, a chip with high efficiency and power up to 10 W for a supply range from 85 V to 265 V. The switching circuit has built-in protections against overcurrent, overvoltage, over-temperature in the switching IC and an auto-restart in case of failure.

The isolation of the primary with the secondary is carried out by the transformer and the feedback circuit which has an opto-coupler to maintain the isolation. The output voltage regulation uses a 3.9 V Zener diode and 1% stability as a reference, which guarantees a maximum variation of the source output voltage in the order of 5%, an acceptable value since the main ICs used in the prototype are powered by isolated DC-DC converters and an output at 3.3 V and a 1% tolerance.

Unlike the other boards of the device, the source board was developed in a single face. The option to mount this board on a single face is due to the fact that it was developed with components in a pin through-hole (PTH) and an SMD, whose production cost is relatively lower.

2.5. Load Control Circuit

For the interface between the ESP32® microcontroller module that operates at 3.3 V and the electronic load triggering device, it was necessary to use an opto-coupler with TRIAC output and zero-cross function. In addition to galvanically isolating the power part from the processing part, the opto-coupler always performs the switching of the load when the electrical network crosses zero, thus ensuring the lowest noise level and current peak.

The board also has a snubber circuit to attenuate the TRIAC switching noise. In order to reduce the final size of the device, the connected load was limited to a single-phase up to 240 V and 10 A. In this way, the heat dissipation of the load actuation device is carried out in the area created for dissipation in the board layout.

2.6. Device Mounting

The device was designed to be mounted as a folding box, with the base being the measurement board, the drive on the sides, the power supply and isolation boards and the processing and communication board as a cover. In this way it was possible to optimize the size end of the device without losing functionality or giving up security and isolation between the measurement board and the processing board. After soldering the components on their respective boards, they were assembled together, resulting in the device illustrated in Figure 4A. In Figure 4B it can be seen that the assembly fit perfectly into the packaging

selected for the meter. A standard DIN rail box was used, which only had to be opened on one side to allow access to the measurement board terminals.

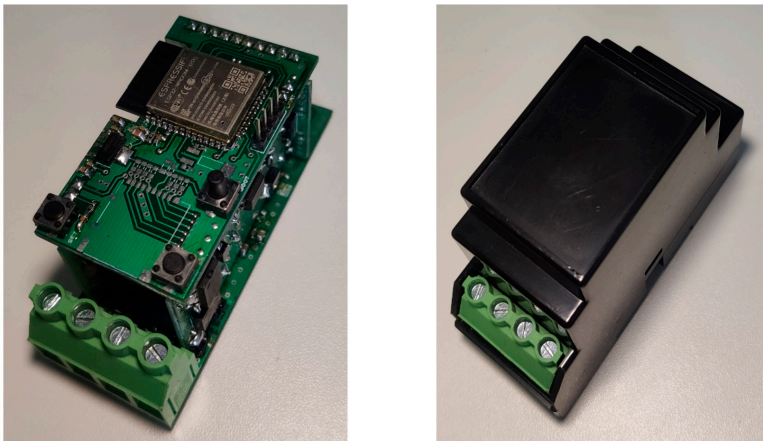

(**A**) (**B**)

Figure 4. Assembly statement (**A**) of the plates and (**B**) in the DIN box.

2.7. Firmware

The firmware embedded in the microcontroller is capable of configuring the energy meter chip, reading all electrical quantities available in the registers, performing the device self-calibration procedure, communicating via a wireless internet network to make the measured data available, and enabling control of the load to the connected device.

The ADE9153A® settings during system startup allow translation of code register values to actual values. This translation is performed through multiplication equations of the values read in the registers, by the target conversion constants. Registry settings are common to each power meter, including thresholds, modes, and architectural requirements such as the value of the shunt resistor and resistive divider.

There are also some registry settings that must be unique for each energy metering device. The values of these records are obtained with the self-calibration process, which has two phases.

The architecture phase, which helps to select component values for design configurations and the production flow phase, is performed on each manufactured device.

Two types of conversion constants are used: (i) the target conversion constant, which is identical for all devices in a given project and (ii) the mSure® conversion constant, which varies from device to device.

The self-calibration process consists of starting the current and voltage reading channel registers so that the mSure® system performs the convergence calculations to obtain the mSure® conversion constants for each channel. This direct signal measurement process does not require a reference meter, the only requirement is that the device is powered and the advanced metrology feature set WATT, VAR, VA, Wh, VARh, and VAh will meet IEC active power standards 62053-21; IEC 62053-22; IEC 50470-3; OIML R46; and ANSI C12.20, as well as the IEC 62053-23 and IEC 62053-24 standards for reactive power and RMS measurement of current and voltage guaranteeing Class 1 measurement in all quantities [27].

The network management was implemented using the native libraries for ESP32® in which the communication between the server and the installed IoT platform takes place through the MQTT protocol.

2.8. Dashboard

The ThingsBoard.io® platform management system configured in a virtual machine instance on Google Cloud® makes it possible to register the devices with which it will communicate, so that each registered device is individually accessed to read the measured data, in addition to allowing the control of the load connected to the respective device. To perform the management functions, access to the server uses the domain or IP address.

To facilitate device management and scalar platform control, it is possible to register devices at any time by accessing the platform settings menu. The addition of the new device is very simplified, whereby an individual just clicks on add, they enter a name for the device and the system automatically generates a security token for its authentication.

According to the need of the application, it is possible to dismember the registration of devices in profiles creating access rules. It is also possible to import a list of devices for mass registration.

According to the desired application of the device, client management can be executed and configured so that the dashboard is accessible from any computer or smartphone with Internet access, with the option of making it public or private. If it is private, it is necessary to register the system's customer and their due level of permissions.

Within the customer management system, it is possible to register the login and password to access the system and link the registered devices that the customer has access to and the dashboard available for the same.

In this way, it is possible to limit the level of access and control of each user. An example would be to customize the dashboard to be only used for monitoring, making it impossible for a given user to disconnect the load connected to the device.

After registering the device and the client with the proper permissions, it is able to feed the telemetry data to the dashboard, starting the process of monitoring and controlling the load. In the identification bar, there are options common to all widgets, such as measurement source device, time window and full screen options. According to the sequence in Figure 5, there are the widgets of (i) control; (ii) RMS voltage; (ii) RMS current; (iv) frequency; (v) measurement board temperature; (vi) power factor; (vii) graphs of active and reactive powers; (viii) measurements of electrical energy consumption; (ix) RMS voltage graph; and (x) RMS current graph.

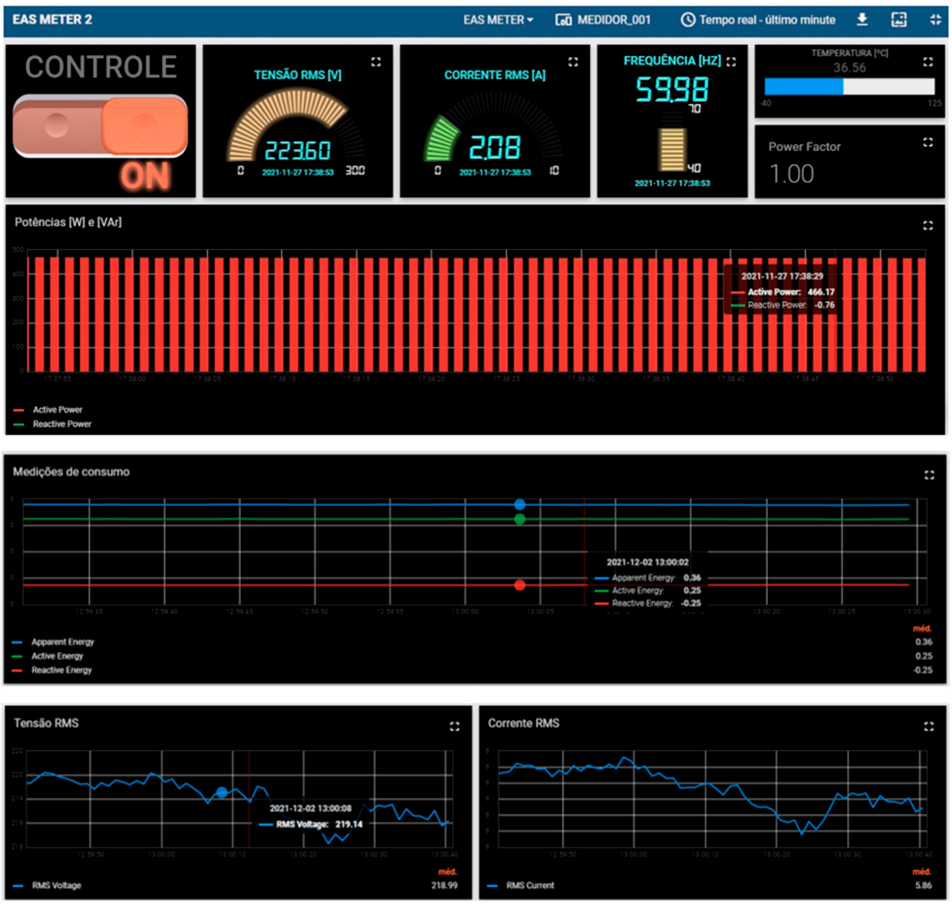

Figure 5. Dashboard of the EAS METER.

The widgets are dynamic and automatically adjust to the size of the screen used, ordering them according to the configuration performed, whether on a desktop, notebook, tablet, or smartphone. To view all widgets, an individual just uses the scroll bar.

2.9. Household Energy Consumption Forecasting

The existence of household energy consumption demand data is relevant for several reasons. These data are helpful in developing methods to promote the quality and continuity of power generation, as well as to secure and meet the growth in residential electricity consumption [28]. In addition, consumption and future prediction information on the demand side is useful when using renewable energies, such as solar photovoltaic and wind energies, which have characteristic intermittencies in their generation process [29].

In this context, one of the indirect contributions of the EAS METER system proposed in this study contemplates its application for the construction of datasets to record energy consumption on the demand side, which can be used in the future to fill the gap of a lack of data and information on household energy consumption in countries such as Brazil [30]. It is important to highlight that the inexistence of these data is a challenge in the scientific literature on household energy consumption prediction (HECF) [31]. Therefore, besides enabling the construction of new datasets, a demand-side HECF module was developed, evaluated, and integrated into the EAS METER prototype developed in this study.

The experimental HECF module aims to predict the residential electricity consumption 10 min ahead using an artificial intelligence model built from historical household energy consumption data. For this, the data from the Almanac of Minutely Power dataset Version 2 (AMPds2) [31] was used, which provides eleven types of electricity-related measurements. Therefore, in this study, the date, time, electricity consumption (kWh), current (I), and temperature (T) of a domestic residence located in Canada were considered. These measurements comprise a historical period of 730 days from April/2012 to March/2014 with samples were recorded every 1 min. In this study we chose the 10 min ahead prediction horizon for the experimental analysis of the HCPF module. It should be noted that the AMPds2 dataset was built especially for the development of research with machine learning algorithms [30]. This study applied the 3-fold cross-validation technique in training the prediction models (Table 1).

Table 1. Dataset split strategy (3-fold) adopted in this study.

Folds	Period (Year/Month)		
	2012/04 TO 2012/11	**2012/12 to 2013/07**	**2013/08 to 2014/03**
Fold-1	Train *	Train	Test
Fold-2	Train	Test	Train *
Fold-3	Test	Train *	Train

* The last (30) thirty days of data were used as the validation set.

Several proposals with different approaches have been reported in the HECF scientific literature [28]. In this study we applied two prediction models based on the Artificial Neural Network (ANN) and Long Short-Term Memory (LSTM) [8]. These models are widely used in regression problems in the scientific literature, such as HECF [32–34]. The fundamental concepts of operation and structure of both models are depicted in Figure 6 and described below.

The ANNs are similar to the neurons of the human brain which are used to solve problems of approximation, classification, standardization, optimization, and prediction [8]. Figure 6a schematically presents an artificial neuron, where $x_1, x_2, \ldots, x_n$ correspond to the inputs. For each input x_i there is a weight w_i corresponding to the sum of the inputs x_i which is pondered by the weights w_i, and the linear output u, where $u = \sum_i w_i x_i$. The activation output y of the neuron is obtained by applying a function f to the linear output u, denoted by $y = f(u)$.

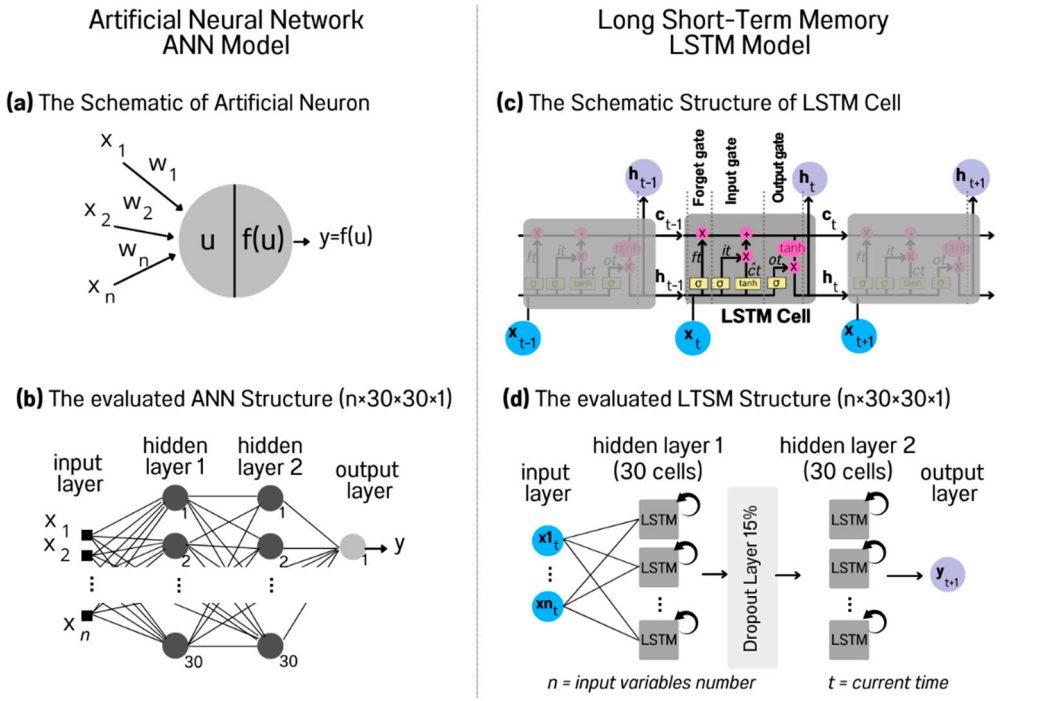

Figure 6. ANN Model: (**a**) an artificial neuron and (**b**) the ANN structure. LSTM model: (**c**) the LSTM cell structure and (**d**) the LSTM structure (the temporal recurrent structure is not shown).

The f function is the activation function and RELu [8] was employed in the ANN model. After the hyperparameter optimization results, the ANN model structure used in this study is depicted in Figure 6b, where the model is composed of n inputs, two hidden layers with 30 neurons each, and a single output neuron y, corresponding to the household energy demand prediction (kWh). The ANN's type adopted in this study are multilayer perceptron (MLP) with the backpropagation training algorithm [8] (Figure 6b).

The other used model is a Long Short-Term Memory (LSTM) which is widely employed for presenting interesting results due to its good ability to deal with the problem of long-term data dependency [35], thus increasing the prediction accuracy [36]. The concepts and LSTM structure adopted in this study are depicted in Figure 6c,d, respectively.

The internal schematic diagram of an LSTM cell is shown in Figure 6c. Considering that W represents a weight and t is the current time [35]:

$$\begin{gathered} f_t = \sigma\left(W_{fh}h_{t-1} + W_{fx}x_t + b_f\right), \\ i_t = \sigma(W_{ih}h_{t-1} + W_{ix}x_t + b_i), \\ \hat{c}_t = tanh(W_{\hat{c}h}h_{t-1} + W_{\hat{c}x}x_t + b_{\hat{c}}), \\ c_t = f_t.c_{t-1} + i_t.\,\hat{c}_t, \\ o_t = \sigma(W_{oh}h_{t-1} + W_{ox}x_t + b_o), \\ h_t = o_t.tanh_{ct} \end{gathered} \tag{1}$$

where x_t is current input, x represents the scaling of information, $+$ is the adding information, σ is the sigmoid function, $tanh$ is the hyperbolic tangent function, h_{t-1} is the output of last LSTM cell, c_t is the new updated memory, h_t is the current output, and f_t, i_t, o_t are the forget, input and output gates, respectively. The general operation focuses on the state of the memory cell flowing through time t¸ with data being received from the previous cell and passed on to the next cell. Additional details of the equations in (1) can be found in [35].

Figure 6d presents the LSTM network architecture evaluated. For the sake of clarity, details of the recursion structure/temporal memory of the LSTM cells have been omitted. The LSTM model has an input layer with n variables, where n is the date, time, and local

temperature. All these data are also provided by the proposed EAS METER system. There are two hidden layers with 30 LSTM cells each, which are interconnected by a dropout layer (15%) to prevent overfitting of the data in the training process [37]. Finally, a single layer with one neuron performs the household energy consumption prediction in kWh, for the next horizon ($t + 1$). For the reproducibility purposes of these models, the main hyperparameters values used in both ANN and LSTM networks are presented in Table 2. It is important to note that the structure and parameter values in this study were defined based on grid search strategy [38].

Table 2. Hyperparameters values used in the ANN and LSTM models.

ANN Model		LSTM Model	
Parameter	**Value**	**Parameter**	**Value**
Activation Function	ReLU	Activation Function	TanH
Epochs	1000	Dropout	0.15
Learn Rate	0.001	Epochs	1000
Total Neurons	60	Learn Rate	0.001
Hidden Layers (HL)	2	Total Cells	60
Neurons in each HL	30	Hidden Layers (HL)	2
		Cells in each HL	30
		Dropout Layer Percentage	0.15

The prediction accuracy of the ANN and LSTM models on the test dataset (25%) was evaluated with the following error metrics commonly used in the literature [29]: coefficient of determination (R^2), mean absolute error (MAE), and root mean square error (RMSE), detailed in Equations (2)–(4), respectively:

$$R^2 = 1 - \frac{\sum_{i=1}^{N}(o_i - p_i)^2}{\sum_{i=1}^{N}(o_i - \mu)^2} \quad (2)$$

$$MAE = \frac{1}{N}\sum_{i=1}^{N}|o_i - p_i| \quad (3)$$

$$RMSE = \sqrt{\frac{1}{N}\sum_{i=1}^{N}(o_i - p_i)^2} \quad (4)$$

In these error metrics, N represents the number of data points in the distribution, M refers to the mean of the observed distribution, p_i to the i_{th} predicted point o_i represents the o_{th} observed point, and μ is the arithmetic mean of o_i [39]. Finally, the best prediction model was adopted in the HECF module of the EAS METER prototype. These results are described in Section 3.9.

3. Experimental Results and Discussion

To validate the functionality of the prototype, an evaluation board from the manufacturer was also acquired. The EV-ADE9153ASHIELDZ® was connected to the Arduino UNO® to make the data available through the serial connection.

Using mSure® automatic calibration, the evaluation board can be self-calibrated, and the manufacturer guarantees to measure energy with 1% accuracy in the dynamic range without the need for calibration equipment.

Since the manufacturer provides the evaluation board's communication library, the validation of the prototype after the execution of the self-calibration was performed by comparing the results obtained in the readings when the same load levels were applied.

The order of validation of the quantities was: (i) RMS voltage; (ii) RMS current; (iii) frequency; (iv) active and reactive power and PF; and (v) active and reactive energy

consumption. Finally, the device was validated in the case of actual installation of use and the cost survey for production was presented.

3.1. RMS Voltage

To carry out the voltage measurement tests, a single-phase voltage regulator with a proportional output of up to 260 V was used. Due to the operating range of the developed switching power supply, the voltage measurement took place from 90 V to 250 V. Table 3 shows the values of the ten readings performed within the device's operating range.

Table 3. Validation of RMS voltage reading.

Test	VARIAC [V]	EVAL [V]	EASMETER [V]	ERROR [%]
1	90.0	89.9	90.0	−0.11
2	100.0	100.0	100.1	−0.10
3	110.0	109.9	110.0	−0.09
4	120.0	119.9	120.0	−0.08
5	130.0	130.1	130.0	0.08
6	190.0	189.9	190.0	−0.05
7	200.0	200.1	200.1	0.00
8	220.0	220.1	220.0	0.05
9	240.0	239.9	240.0	−0.04
10	250.0	249.9	249.8	0.04

The voltage value of the single-phase voltage regulator was checked with a UNI-T® device, model UT210E PRO® which has a 1% accuracy in the measured range, and, as can be seen, the largest error was 0.2 V, practically at the bottom of the scale, thus assigning an error of 0.08% in comparison with the evaluation board.

3.2. RMS Current

To carry out the current measurement tests, a halogen space heater, a hair dryer, and an electric grill were used as the load. The heater used has two heating stages and the loads were combined to cover 0 A to 10 A operating range of the current in the device. In Table 4, the values obtained are presented and it is possible to observe that, as in the voltage measurements, the difference between the measurements is minimal, with the maximum discrepancy between the values being 0.01 A, that is, 0.1% at the bottom of scale.

Table 4. Validation of RMS current reading.

Load	UT210EPRO [A]	EVAL [A]	EASMETER [A]	ERROR [%]
1	1.09	1.10	1.09	0.91
2	2.15	2.15	2.14	0.47
3	4.29	4.29	4.28	0.23
4	6.45	6.45	6.44	0.16
5	8.58	8.59	8.58	0.12
6	10.64	10.63	10.64	0.00

During the execution of this test, the overcurrent protection triggering setting was determined, as the device must work up to 10 A. If the reading taken exceeds the value configured as the overcurrent limit, the load is turned off in the next measurement cycle. The validation of this protection was carried out with the data obtained by the debug terminal used during the tests and it was verified that in the measurement cycle after the identification of the overcurrent, the device performed the load cut.

3.3. Frequency

Frequency measurement considers the period of the voltage signal that has its value available in the APERIOD register of the energy measurement IC. If the value of the calculated period is out of range, i.e., it is not between 40 Hz and 70 Hz or zero crossings are not detected in the voltage signal, this fault is observed through the interruption generated by the timeout overflow of the zero-crossing register.

The validation of the frequency readings took place by comparing the value shown on the panel accessed on a cell phone with the value indicated by the UT210E PRO®, in operation at 60 Hz. As expected, this value was identical to the measured one and dynamically followed its variations.

3.4. Active, Reactive Powers and PF

To validate the active power, the space heater of the electric current tests was used as a load and the values obtained on the dashboard were compared with the values read by the evaluation board.

Through calculating the active power value by multiplying the RMS voltage and current values, 898.33 W is obtained, which represents a difference of 0.17% in relation to the active power value measured by the prototype. When compared to the evaluation board, the error percentage reduces to 0.04%.

To validate the reactive power, a capacitive load used in power factor correction was used as a load, in addition to the space heater of the electric current tests, and the values obtained on the dashboard were compared with the values read by the evaluation. The error presented is 0.02 Var, that is, a percentage error in relation to the measurement of the evaluation board of 0.002%.

Subsequently, the capacitive load was replaced by an inductive load, and it was also possible to validate the power factor, which, as a consequence of dividing the active power by the apparent power, did not present a considerable error due to the precision of the previous validated measurements.

3.5. Active and Reactive Energy Consumption

In the same test, following the measurement of the quantities, the integration of the sixty-second measurements of active and reactive energy was carried out, according to the export of the telemetry bank created for the dashboard.

Data export was designed to enable integration with commercial systems. In this way, each variable could be requested through commands to the server, which creates a list with the timestamp in milliseconds in a Unix format and the value of the requested magnitude. This list is available in .csv format as it is easily converted to any other format.

To simulate commercial software, a simple Python® terminal was developed, which makes the request to the server and records the file available with the start and end times of the telemetry. After downloading the file, with the integration of the prototype's active and reactive energy values and comparing them with the integration presented by the evaluation board, an error of 0.04% is observed in both quantities.

3.6. Device Validation in a Real Installation

After the individual validation of the quantities and with the prototype presenting the readings within the expected values in the laboratory, it was installed in an apparent distribution board of a residence. The external lighting of the residence was divided into two circuits and added to the prototypes to be controlled and monitored by the devices.

Circuit one controls three front garden lighting reflectors, each reflector with a power of 50 W. Circuit two controls the patio lighting, consisting of four 14 W LED lamps and two 50 W reflectors. In this way, it is possible to read the magnitudes of each circuit as well as the activation and disconnection of loads via the Internet.

With the system integrated and operating continuously, it was possible to use it to manage the loads in operation, as well as to collect data in the field in an automated and

accurate way. In this way and with the integration with existing commercial software, the analysis and automatic proposal of energy efficiency actions for the various end uses and the issuance of reports of different types were simplified.

3.7. Production Costs

The survey of costs for scale production of the device was divided into the component and assembly costs. It is possible to observe from Table 5 that the cost for mass production suffers a considerable reduction.

Table 5. Mass production cost.

Individual Cost for Unit (US$)	10 Unit	100 Unit	1000 Unit	10,000 Unit
Electronic component cost	48.98	40.84	34.96	28.10
2 DIN plastic box	1.91	1.59	1.36	1.10
Printed circuit board	5.29	4.41	3.78	3.04
SMD mounting	6.36	5.30	4.54	3.65
Total	62.54	52.15	44.64	35.88

The acquisition costs of electronic components represent the greatest value due to the high added cost of import, however it is possible with scale production to seek a reduction in tax values and even some subsidies for maintenance of the production of devices.

Compared to competing pieces of equipment on the market, the cost is competitive, since it is the lowest cost at a large scale. In addition, it delivers more functionality than other devices available on the Brazilian market and contemplates a differentiated solution through the scalability of the management and monitoring system [40–42].

3.8. Technical Characteristics

To complete the job and with the current configuration of the device, the technical characteristics are presented in Table 6. However, they can be adapted according to the need of the solution sought through the constant evolution of the development and production of new versions.

Table 6. Technical characteristics of the device.

Voltage	Operating range from 85 V to 275 V (phase-to-neutral voltage)
Current	Maximum Current 10 A
Frequency	From 40 to 70 Hz
Accuracy	Class 1 (1% for all measured quantities)
Sampling rate	4000 SPS
Temperature range	De −10 °C a 70 °C
Communication interfaces	802.11 b/g/n (802.11 n até 150 Mbps)
Measured quantities	V, I, HZ, WATT, VAR, VA, FP, Wh, VARh, e VAh
Dimensions	88 × 37 × 59 mm
Weight	0.6 kg

Therefore, in addition to being a piece of equipment developed for monitoring consumption, the device demonstrated herein can also be used for diagnosis and studies in the area of efficiency and energy conservation. In Brazil, according to the national electric energy agency, the measurement and verification protocol is used to determine energy efficiency improvements. Therefore, this device ends up filling the gap in the availability of equipment for such a function that is, in addition, easy to use and install.

3.9. Accuracy of Energy Consumption Forecasting

This section presents the prediction accuracy results of the HECF module considering the ANN and LSTM models for integration into the EAS METER prototype. In order to establish a comparative baseline reference of the predictions, the prediction accuracy for the Persistence (or baseline) model [43] is also presented. The Persistence method is simple and assumes that the system state (electricity consumption in this case) remains the same between time instants t and $t + h$, where t is the current time and h is the next measurement time [43].

Table 7 and Figure 7 display the results of the average accuracy and standard deviation (SD) for the R2, MAE, and RMSE values of the predictions of the Persistence, ANN and LSTM models. Test data from the 3-fold cross-validation are presented for each model. The accuracy of the Persistence model is much lower compared to the MLP and LSTM models and is therefore not mentioned in the analyses (Table 7). For all of the metrics and folds, the average prediction accuracy of the LSTM models outperforms the ANNs by approximately 44.3% (MAE) and 52.2% (RMSE) (Figure 7, right). This shows that the LSTM models better captured the pattern and temporal variability of the residential electric consumption data (HPCF). Possibly, this is due to the ability of LSTMs to memorize the long-term temporal dependencies in the historical [44] household energy consumption data captured and available by the EAS METER.

Table 7. The HPCF accuracy for both ANN and LSTM evaluated models in the EAS METER.

Model	Accuracy	Fold-1	Fold-2	Fold-3	Mean	SD
Persistence	R^2	0.31	0.37	0.25	0.31	0.06
	MAE	396.14	376.22	385.12	385.83	9.98
	RMSE	804.50	764.92	770.93	780.12	21.33
ANN	R^2	0.99	0.99	0.99	0.99	0.00
	MAE	11.87	13.51	15.82	13.73	1.98
	RMSE	21.01	30.48	28.68	26.72	5.03
LSTM	R^2	0.99	0.99	0.99	0.99	0.00
	MAE	7.50	8.69	6.74	7.64	0.98
	RMSE	12.29	14.71	11.29	12.76	1.76

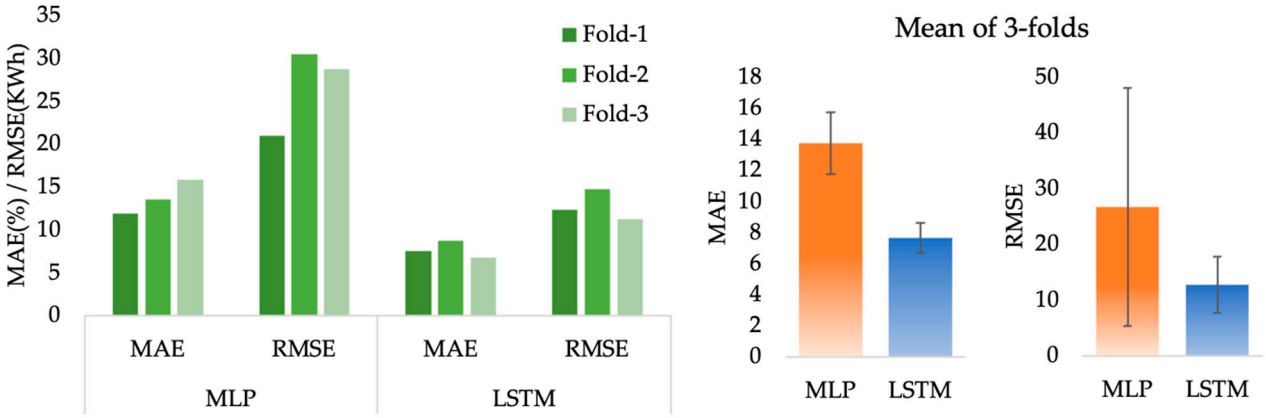

Figure 7. Accuracy results of MLP and LSTM models in each fold (**left**). Mean errors of MAE and RMSE with standard deviation (SD) of MLP and LSTM models (**right**).

Although the main objective of this study was to present the development of the EAS METER prototype, it has been highlighted that it was not aimed at optimizing the accuracy of the predictions of residential energy consumption with the HPCF module developed in

this study. However, it was highlighted that the results of the LSTMs models, in the HPCF module, exhibit prediction accuracy values for 10 min ahead, which is similar to other studies in the literature [33,34], thus demonstrating them to be applicable and suitable for the prediction of household energy consumption from data generated by the proposed EAS METER prototype. Figure 8 displays examples of the predictions for the 10 min horizon for one particular day (4 October 2012) from the models evaluated in this study.

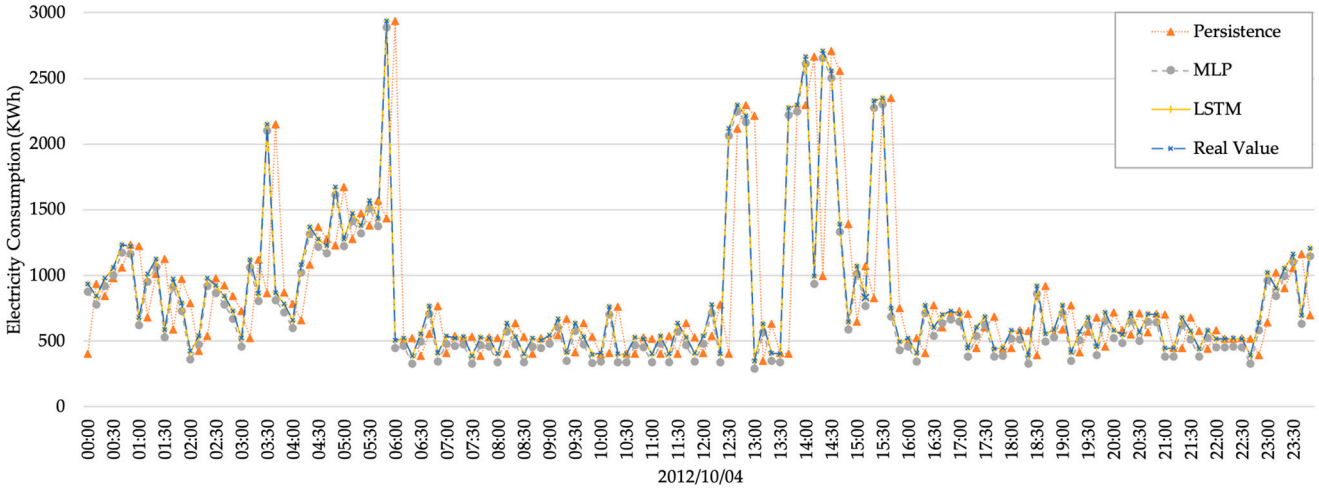

Figure 8. Examples of electricity consumption predictions of HCPF module for one day.

Finally, we emphasize that the insertion of the HPCF module to EAS METER adds an additional functionality that facilitates the development of future studies regarding the prediction of energy consumption on the demand side, considering different regional profiles of residential energy consumption. The capture of these data in real time by EAS METER facilitates and promotes the proposition and optimization of new HCPF techniques. It is noteworthy that the measurement and load monitoring are performed through edge computing on the ADE9153A and EPS32 devices. On the other hand, the dashboard and the household energy consumption prediction (HECF) module provide access to this information using Google Cloud Platform® cloud computing services.

4. Conclusions

The main result of this work was the development of a prototype with a high level of hardware and software integration, including the differential characteristic of autocalibration. In addition, as specified by the manufacturer of the measurement IC used, the device has an advanced metrology feature set included as WATT, VAR, VA, Wh, VARh, and VAh. It also supports the active energy standards: IEC 62053-21; IEC 62053-22; EN50470-3; OIML R46; and ANSI C12.20, and reactive energy standards as well: IEC 62053-23 and IEC 62053-24 for current and voltage RMS measurement and power quality measurements.

It is important to emphasize that the main focus of the contribution of this study was the development of the self-calibrated embedded system that makes it possible to measure, control, and predict the consumption of domestic electrical loads, with emphasis on the use of the ADE9153A device, dispensing with the need for an additional specific calibrated meter. The mSure® autocalibration feature allows a meter to automatically calibrate the current and voltage channels without using an accurate source or an accurate reference meter when a shunt resistor is used as a current sensor. Class 1 m are supported by mSure autocalibration. Therefore, this feature reduces calibration and certification costs by dispensing with standard reference meters, which are often extremely expensive or have calibration costs in external laboratories. In addition, this feature simplifies the process of production and testing of equipment in the production line.

According to the validations carried out, the device proved to be efficient in the operating range from 90 V to 250 V, as the implemented source is within a universal range,

the operating voltage does not need to be selected in the device, and it has the possibility of measuring currents of up to 10 A, equivalent to the switching threshold supported by the device. It was possible to verify too that all the measured quantities which presented measurement errors were smaller than 1% of the full scale and that, in the production scale, the parameterization process of the devices was simplified.

It should be noted that the sampling rate of the EAS METER prototype depends on the scale that is selected. The DSP has a processing capacity of 4kSPS, i.e., 4000 samples per second. This sampling is configurable and in this study the period of one minute was considered. However, the volume of data enables more refined analysis compared to a device with an integration time of more minutes. The residential energy consumption prediction functionality (HPCF module) provided in the EAS METER prototype demonstrated acceptable accuracy using LSTM models (MAE = 7.64 and RMSE = 12.76) for 10 min ahead prediction. In addition to the real-time energy consumption data captured by the EAS METER, the prediction horizon of the HPCF module can be expanded in the future for use by electric management operators where, for example, day-ahead or long-term prediction models can be developed and added to the EAS METER to make predictions from real-time captured data.

In addition, another indirect contribution of the EAS METER system contemplates its application for the construction of new datasets regarding energy consumption on the demand side, including capturing data in real time. It is important to note that this information is scarce or non-existent in some countries, such as Brazil [30], and its availability is necessary for planning, management, and operation in distributed systems of renewable energy generation, such as photovoltaic or wind power. For example, household energy consumption profile data can be used by renewable energy (photovoltaic or wind) generation prediction systems to mitigate the effects of power generation intermittencies as a function of energy consumption on the demand side [29,45,46].

It is worth mentioning that the final cost of the device was below 300 BRL (i.e., around 60 USD at the current exchange rate) and that the device can be used in numerous applications such as: a load curve survey; to generate the consumption history and make it possible to improve the prediction of future loads on consumers; to create datasets from households' power consumption and demand to be used as benchmarks in machine learning models in future studies; to create awareness for energy users; to provide remote control of single-phase loads; to provide in addition measurement and verification systems to validate the implementation of energy efficiency systems.

Author Contributions: Conceptualization: E.A.d.S. and O.H.A.J.; investigation and simulation: E.A.d.S., C.A.U., J.N.M. and O.H.A.J.; writing and final editing: E.A.d.S., J.J.G.L., M.R.C. and O.H.A.J. All authors have read and agreed to the published version of the manuscript.

Funding: This research was funded by the Federal University of Latin American Integration (UNILA). O.H.A.J. was funded by the Brazilian National Council for Scientific and Technological Development (CNPq), grant number 407531/2018-1 and 303293/2020-9.

Institutional Review Board Statement: Not applicable.

Informed Consent Statement: Not applicable.

Data Availability Statement: Data are contained within this study.

Acknowledgments: The authors would like to thank the Federal University of Latin American Integration (UNILA), the Federal Rural University of Pernambuco (UFRPE) for financial supporting and facilities, the Coordination for the Improvement of Higher Education Personnel (CAPES) and the Brazilian Council for Scientific and Technological Development (CNPq) for financial support.

Conflicts of Interest: The authors declare no conflict of interest.

Nomenclature

ADC	Analog-to-digital Converter
AI	Artificial Intelligence
ANN	Artificial Neural Network
BLE	Bluetooth Low Energy
DIN	Deutsches Institut für Normung
GCP	Google Cloud Platform
HECF	Household Energy Consumption Forecasting
IC	Integrated circuit
INPI	Brazilian National Institute of Industrial Property
IoT	Internet of Things
LSTM	Long Short-Term Memory
MAE	Mean Absolute Error
M2M	Machine-to-Machine
MQTT	Message Queue Telemetry Transport
NZEB	Near Zero Energy Buildings
PTH	Pin Through Hole
QoS	Quality of Service
RF	Radio frequency
RMS	Root Mean Square
RMSE	Root Mean Squared Error
R^2	Coefficient of Determination
SMD	Surface Mounted Device
SPI	Serial Peripheral Interface
SD	Standard Deviation
UART	Universal Asynchronous Receiver Transmitter

References

1. Jia, M.; Komeily, A.; Wang, Y.; Srinivasan, R.S. Adopting Internet of Things for the development of smart buildings: A review of enabling technologies and applications. *Autom. Constr.* **2019**, *101*, 111–126. [CrossRef]
2. Amaral, H.L.M.D.; De Souza, A.N.; Gastaldello, D.S.; Fernandes, F.; Vale, Z. Smart meters as a tool for energy efficiency. In Proceedings of the 2014 11th IEEE/IAS International Conference on Industry Applications, IEEE Indusconic 2014—Electronic Proceedings, Juiz de Fora, Brazil, 7–10 December 2014. [CrossRef]
3. Shibu, N.B.S.; Hanumanthiah, A.; Rohith, S.S.; Yaswanth, C.; Krishna, P.H.; Pavan, J.V.S. Development of IoT Enabled Smart Energy Meter with Remote Load Management. In Proceedings of the 2018 IEEE International Conference on Computational Intelligence and Computing Research, ICCIC 2018, Madurai, India, 13–15 December 2018; pp. 1–4. [CrossRef]
4. Ahmad, M.W.; Mourshed, M.; Mundow, D.; Sisinni, M.; Rezgui, Y. Building energy metering and environmental monitoring—A state-of-the-art review and directions for future research. *Energy Build.* **2016**, *120*, 85–102. [CrossRef]
5. Nižetić, S.; Djilali, N.; Papadopoulos, A.; Rodrigues, J.J. Smart technologies for promotion of energy efficiency, utilization of sustainable resources and waste management. *J. Clean. Prod.* **2019**, *231*, 565–591. [CrossRef]
6. Siano, P. Demand response and smart grids—A survey. *Renew. Sustain. Energy Rev.* **2014**, *30*, 461–478. [CrossRef]
7. Daissaoui, A.; Boulmakoul, A.; Karim, L.; Lbath, A. IoT and Big Data Analytics for Smart Buildings: A Survey. *Procedia Comput. Sci.* **2020**, *170*, 161–168. [CrossRef]
8. Shaukat, N.; Ali, S.; Mehmood, C.; Khan, B.; Jawad, M.; Farid, U.; Ullah, Z.; Anwar, S.; Majid, M. A survey on consumers empowerment, communication technologies, and renewable generation penetration within Smart Grid. *Renew. Sustain. Energy Rev.* **2018**, *81*, 1453–1475. [CrossRef]
9. Avancini, D.B.; Rodrigues, J.J.; Martins, S.G.; Rabêlo, R.A.; Al-Muhtadi, J.; Solic, P. Energy meters evolution in smart grids: A review. *J. Clean. Prod.* **2019**, *217*, 702–715. [CrossRef]
10. Haider, H.T.; See, O.H.; Elmenreich, W. A review of residential demand response of smart grid. *Renew. Sustain. Energy Rev.* **2016**, *59*, 166–178. [CrossRef]
11. Shrouf, F.; Miragliotta, G. Energy management based on Internet of Things: Practices and framework for adoption in production management. *J. Clean. Prod.* **2015**, *100*, 235–246. [CrossRef]
12. Pagani, R.N.; Kovaleski, J.; Resende, L.M. Methodi Ordinatio: A proposed methodology to select and rank relevant scientific papers encompassing the impact factor, number of citation, and year of publication. *Scientometrics* **2015**, *105*, 2109–2135. [CrossRef]
13. Abate, F.; Carratu', M.; Liguori, C.; Paciello, V. A low cost smart power meter for IoT. *Measurement* **2019**, *136*, 59–66. [CrossRef]

14. Minchev, D.P.; Dimitrov, A.I. Laboratory Automation System Using IOT Devices. In Proceedings of the 2020 21ST International Symposium on Electrical Apparatus & Technologies (SIELA), Anais IEEE, Bourgas, Bulgaria, 3–6 June 2020; pp. 1–4. Available online: https://ieeexplore.ieee.org/document/9167121/ (accessed on 4 September 2020). [CrossRef]
15. Athanasiadis, C.; Doukas, D.; Papadopoulos, T.; Chrysopoulos, A. A Scalable Real-Time Non-Intrusive Load Monitoring System for the Estimation of Household Appliance Power Consumption. *Energies* **2021**, *14*, 767. [CrossRef]
16. Athanasiadis, C.L.; Papadopoulos, T.A.; Doukas, D.I. Real-time non-intrusive load monitoring: A light-weight and scalable approach. *Energy Build.* **2021**, *253*, 111523. [CrossRef]
17. Yelisetti, S.; Saini, V.K.; Kumar, R.; Lamba, R.; Saxena, A. Optimal energy management system for residential buildings considering the time of use price with swarm intelligence algorithms. *J. Build. Eng.* **2022**, *59*, 105062. [CrossRef]
18. Lucchi, E.; Pereira, L.D.; Andreotti, M.; Malaguti, R.; Cennamo, D.; Calzolari, M.; Frighi, V. Development of a Compatible, Low Cost and High Accurate Conservation Remote Sensing Technology for the Hygrothermal Assessment of Historic Walls. *Electronics* **2019**, *8*, 643. [CrossRef]
19. Charoen, P.; Kitbutrawat, N.; Kudtongngam, J. A Demand Response Implementation with Building Energy Management System. *Energies* **2022**, *15*, 1220. [CrossRef]
20. Saraiva, J.; Machado, W.V.; Bazi, F.d.C.; Saraiva, J.L.S.; de Seixas, P.R.B. Dispositivo Integrado Com Sistema De Gestão, Automação, Monitoramento, Controle De Consumo E Qualidade De Energia Elétrica Para Quadros De Distribuição Elétrica Residencial, Comercial E Industrial Baseado Em Internet Das Coisas. BR 10 2019 023392 3, 10 November 2020.
21. De Araújo, A.L.C.; Filho, R.G.D.; de Albuquerque, A.A.M.; Lima, P.R.C.; Cardoso, H.N.d.S. Sistema Para Gerenciamento Remoto De Cargas Elétricas. BR 10 2018 017224 7, 3 March 2020.
22. Sandi, T. Dispositivo E Sistema Para Monitoramento Da Eficiência De Equipamentos Elétricos. BR 10 2017 025250 7, 11 June 2019.
23. Junior, O.H.A.; Bretas, A.S.; Leborgne, R.C. Methodology for Calculation and Management for Indicators of Power Quality Energy. *IEEE Lat. Am. Trans.* **2015**, *13*, 2217–2224. [CrossRef]
24. Goodfellow, I.; Bengio, Y. *Aaron Courville Deep Learning*; MIT Press: Cambridge, MA, USA, 2016.
25. Espressif. ESP32 Technical Reference ManualUS Army Corps of Engineers. [s.l: S.n.]. Available online: https://www.espressif.com.cn/sites/default/files/documentation/esp32_technical_reference_manual_en.pdf (accessed on 4 September 2020).
26. Analog Devices, Inc. *EV-ADE9153ASHIELDZ User Guide EV*; Analog Devices, Inc.: Wilmington, MA, USA, 2018.
27. Analog Devices, Inc. *Energy Metering IC with Autocalibration ADE9153A*; Analog Devices, Inc.: Wilmington, MA, USA, 2018.
28. Zhou, K.; Yang, S. Understanding household energy consumption behavior: The contribution of energy big data analytics. *Renew. Sustain. Energy Rev.* **2016**, *56*, 810–819. [CrossRef]
29. Maciel, J.N.; Ledesma, J.J.G.; Junior, O.H.A. Forecasting Solar Power Output Generation: A Systematic Review with the Proknow-C. *IEEE Lat. Am. Trans.* **2021**, *19*, 612–624. [CrossRef]
30. Lima, C.A.F.; Gomes, R.D.M.; Maciel, A.A. *Uso de Novas Tecnologias Digitais Para Medição de Consumo de Energia e Níveis de Eficiência Energética No Brasil—Baseado Nas Experiências Da Alemanha*; Deutsche Gesellschaft für Internationale Zusammenarbei: Brasília, Brazil, 2021.
31. Makonin, S.; Ellert, B.; Bajić, I.V.; Popowich, F. Electricity, water, and natural gas consumption of a residential house in Canada from 2012 to 2014. *Sci. Data* **2016**, *3*, 160037. [CrossRef]
32. Feurer, M.; Hutter, F. Hyperparameter Optimization. In *Studies in Computational Intelligence*; Hutter, F., Kotthoff, L., Vanschoren, J., Eds.; The Springer Series on Challenges in Machine Learning; Springer International Publishing: Cham, Switzerland, 2019; Volume 498, pp. 3–33. ISBN 978-3-030-05317-8.
33. Sajjad, M.; Khan, Z.A.; Ullah, A.; Hussain, T.; Ullah, W.; Lee, M.Y.; Baik, S.W. A Novel CNN-GRU-Based Hybrid Approach for Short-Term Residential Load Forecasting. *IEEE Access* **2020**, *8*, 143759–143768. [CrossRef]
34. Zhang, C.; Li, J.; Zhao, Y.; Li, T.; Chen, Q.; Zhang, X. A hybrid deep learning-based method for short-term building energy load prediction combined with an interpretation process. *Energy Build.* **2020**, *225*, 110301. [CrossRef]
35. Yu, Y.; Si, X.; Hu, C.; Zhang, J. A Review of Recurrent Neural Networks: LSTM Cells and Network Architectures. *Neural Comput.* **2019**, *31*, 1235–1270. [CrossRef] [PubMed]
36. Haviv, D.; Rivkind, A.; Barak, O. Understanding and Controlling Memory in Recurrent Neural Networks. In Proceedings of the 36th International Conference on Machine Learning, ICML 2019, Long Beach, CA, USA, 10–15 June 2019; pp. 4733–4741.
37. Srivastava, N.; Hinton, G.; Krizhevsky, A.; Sutskever, I.; Salakhutdinov, R. Dropout: A Simple Way to Prevent Neural Networks from Overfitting. *J. Mach. Learn. Res.* **2014**, *15*, 1929–1958.
38. Yang, L.; Shami, A. On hyperparameter optimization of machine learning algorithms: Theory and practice. *Neurocomputing* **2020**, *415*, 295–316. [CrossRef]
39. Shcherbakov, M.V.; Brebels, A.; Shcherbakova, N.L.; Tyukov, A.P.; Janovsky, T.A.; Kamaev, V.A. evich A Survey of Forecast Error Measures. *World Appl. Sci. J.* **2013**, *24*, 171–176. [CrossRef]
40. Aiolfi, M.; Timmermann, A. Persistence in forecasting performance and conditional combination strategies. *J. Econ.* **2006**, *135*, 31–53. [CrossRef]
41. Hochreiter, S.; Schmidhuber, J. Long short-term memory. *Neural Comput.* **1997**, *9*, 1735–1780. [CrossRef]
42. Santos, A.; da Silva, A.; Ledesma, J.; de Almeida, A.; Cavallari, M.; Junior, O. Electricity Market in Brazil: A Critical Review on the Ongoing Reform. *Energies* **2021**, *14*, 2873. [CrossRef]

43. Dranka, G.G.; Ferreira, P. Towards a smart grid power system in Brazil: Challenges and opportunities. *Energy Policy* **2019**, *136*, 111033. [CrossRef]
44. Russell, S.; Norvig, P. *Artificial Intelligence: A Modern Approach*, 3rd ed.; Pearson Education India: Bengaluru, India, 2015.
45. Crepaldi, J.; Amoroso, M.M.; Ando, O. Analysis of the Topologies of Power Filters Applied in Distributed Generation Units—Review. *IEEE Lat. Am. Trans.* **2018**, *16*, 1892–1897. [CrossRef]
46. Spacek, A.D.; Junior, O.H.A.; Neto, J.M.; Coelho, V.; Oliveira, M.; Shaeffer, L.; Gruber, V. Management of Mechanical Vibration and Temperature in Small Wind Turbines Using Zigbee Wireless Network. *IEEE Lat. Am. Trans.* **2013**, *11*, 512–517. [CrossRef]